Published in final edited form as:
J Biol Chem. 2002 August 2; 277(31): 28038–28050. doi:10.1074/jbc.M202367200.

Functional Reconstitution of Human FcRn in Madin-Darby Canine Kidney Cells Requires Co-expressed Human β_2-Microglobulin

Steven M. Claypool[‡,§], **Bonny L. Dickinson**[¶], **Masaru Yoshida**[§], **Wayne I. Lencer**[¶,‖,**], and **Richard S. Blumberg**[§,‖,**,‡‡]

[‡] Harvard Medical School, Program in Immunology, Boston, Massachusetts 02115

[§] Gastroenterogy Division, Brigham and Women's Hospital, Boston, Massachusetts 02115

[¶] Gastrointestinal Cell Biology and Department of Medicine, Children's Hospital, Boston, Massachusetts 02115

[‖] Harvard Digestive Diseases Center, Boston, Massachusetts 02115

Abstract

The major histocompatibility complex class I-related neonatal Fc receptor, FcRn, assembles as a heterodimer consisting of a heavy chain and β_2-microglobulin (β_2m), which is essential for FcRn function. We observed that, in Madin-Darby canine kidney (MDCK) cells, the function of human FcRn in mediating the bidirectional transport of IgG was significantly increased upon co-expression of the human isoform of β_2m. In MDCK cells, the presence of human β_2m endowed upon human FcRn an enhanced ability to exit the endoplasmic reticulum and acquire mature carbohydrate side-chain modifications at steady state, a faster kinetics of maturation, and augmented localization at the cell surface as a mature glycoprotein able to bind IgG. Although human FcRn with immature carbohydrate side-chain modifications was capable of exhibiting pH-dependent binding of IgG, only human FcRn with mature carbohydrate side-chain modifications was detected on the cell surface. These results show that human FcRn travels to the cell surface via the normal secretory pathway and that the appropriate expression and function of human FcRn in MDCK cells depends upon the co-expression of human β_2m.

Epithelial cells form a cohesive single layer that functions as a barrier to separate the luminal and abluminal tissue compartments. Transcytosis refers to the collective process whereby macromolecules are transported across an epithelial layer. Consistent with the potentially hostile environment intimately associated with many epithelial barriers, the adaptive immune system has harnessed the transcytotic machinery to transport intact antibodies across epithelial cell monolayers through the use of at least two transmembrane receptors, the polymeric immunoglobulin receptor (pIgR)[1] and the MHC class I-related Fc receptor originally defined in neonatal life, FcRn. Significant progress has been made in molecularly characterizing pIgR-dependent transcytosis of dimeric IgA and pentameric IgM in the basolateral to apical direction.

‡‡Supported by NIH Grants DK44319 and DK51362. To whom correspondence should be addressed: Gastroenterology Division, Dept. of Medicine, Brigham and Women's Hospital, Harvard Medical School, 75 Francis St., Boston, MA 02115. Tel.: 617-732-6917; Fax: 617-264-5185; rblumberg@partners.org.
**Supported by National Institutes of Health (NIH) Grant DK53056 and the Harvard Digestive Diseases Center.

[1]The abbreviations used are: pIgR, polymeric immunoglobulin receptor; hβ_2m, human β_2-microglobulin; MDCK, Madin-Darby canine kidney; hFcRn, human FcRn; IMCD, inner medullary collecting duct; EndoH, endoglycosidase H; PNGaseF, peptidyl-*N*-glycanase; MHC, major histocompatibility complex; HA, hemagglutinin; PBS, phosphate-buffered saline; ER, endoplasmic reticulum; RIPA, radioimmune precipitation buffer; CHAPS, 3-[(3-cholamidopropyl)dimethylammonio]-1-propanesulfonic acid; HRP, horseradish peroxidase; β-ME, β-mercaptoethanol; MES, 4-morpholineethanesulfonic acid; HBSS, Hanks' balanced salt solution; ANOVA, analysis of variance.

A large proportion of the work associated with dissecting pIgR cell biology has utilized the polarized Madin-Darby canine kidney (MDCK) cell model stably expressing the rabbit pIgR (1–3). Together with the numerous studies on transferrin receptor trafficking, a detailed characterization of the itineraries traveled by proteins undergoing such processes as basolateral recycling, basolateral to apical transcytosis, and apical recycling has been generated for MDCK cells (4–6). One major area of understanding that is currently lacking, however, is the pathway traversed by proteins trafficking in the apical to basolateral direction. This is mainly due to the lack of a good model protein that physiologically harnesses this pathway. Additionally, the ability to generalize the numerous discoveries made studying pIgR and transferrin receptor trafficking in MDCK cells needs to be directly tested by comparing the cell biology of additional receptor systems, which share similar functional behaviors but which may or may not involve new pathways, sorting signals, or machinery.

Two functions have been attributed to FcRn, both of which depend on the abilities of FcRn to bind IgG at acidic pH (pH $\leq$ 6.5) but not at or above neutral pH (pH $\geq$ 7.0) and traffic in cells (7,8). In adult rodents and, likely, in all mammals, FcRn acts as a saturable catabolic protection receptor critical for the maintenance of normal steady-state IgG levels in the blood (9–13). Second, in suckling mice and rats, FcRn mediates the vectorial transport of maternal IgG from the intestinal lumen across the intestinal epithelial cells into the systemic circulation of the neonate (8,9,14–16). In humans, maternofetal transfer of IgG also depends on FcRn in a manner analogous to the processes described in neonatal rodents (17–21). Thus, FcRn has the *in vivo* capacity to transport IgG in the apical to basolateral direction and is therefore an attractive candidate to model trafficking in this direction. Interestingly, several *in vitro* studies have demonstrated the expanded capacity of FcRn to transcytose in both the apical to basolateral and basolateral to apical directions (22–26), suggesting that FcRn may present to the cell multiple sorting determinants whose hierarchy can be altered to facilitate the complex trafficking behavior of FcRn. Conversely, FcRn may be devoid of any strong sorting signal and detectable IgG transport in any one direction is secondary to either a steep pH and/or IgG concentration gradient.

Although major advances have been made on the interaction of FcRn with its ligand, IgG (27–37), progress in characterizing the cell biology of human and rodent FcRn as expressed in polarized epithelia has been comparatively slow. Although work on endogenously expressed human FcRn (hFcRn) is vital in substantiating the hypothesis that FcRn is a bidirectional transporter (22,23,38), it has the major setback of not allowing the type of structure-function analysis required to dissect where the sorting information of FcRn is contained. A major effort by Simister and colleagues (26,39,40) has focused on characterizing rat FcRn trafficking in the rat inner medullary collecting duct (IMCD) cell line. Two main advantages of utilizing the IMCD cell line to study rat FcRn is that it doesn't express endogenous rat FcRn heavy chain but does express the homologous rat β_2m subunit. This latter fact is an important consideration, because, like most other MHC class I-like receptors, FcRn is expressed as a heterodimer consisting of a glycosylated heavy (α) chain (40 –44 kDa in humans; 48 –50 kDa in rodents) associated non-covalently with β_2m (41,42). Furthermore, the importance of β_2m for FcRn function is highlighted by the dual observations that β_2m co-distributes with FcRn along the entire transcytotic pathway in neonatal rat small intestinal epithelial cells (43) and that in $\beta_2m^{-/-}$ mice, both of FcRn's aforementioned functions are abrogated (10–13,16). However, one disadvantage of the IMCD cell line is that, compared with the MDCK cell system, relatively little is known about the trafficking of other model receptors.

Given that the MDCK cell system is so well characterized, it is an attractive candidate to dissect how FcRn traffics in polarized epithelia. The fact that FcRn is an obligate heterodimer, however, adds a level of complexity beyond simply expressing a heterologous FcRn heavy chain in MDCK cells and that was not addressed in a previous study of hFcRn expressed in

MDCK cells (25). Determining the potential requirement to express the homologous human β_2m (hβ_2m) subunit is of fundamental importance in establishing a model system that would allow a future structure-function approach. The importance of addressing this variable is underscored by the fact that canine β_2m contains a valine at amino acid 1 of the mature protein (44) instead of the isoleucine found in rodents and humans, the exact residue demonstrated to contribute a contact site during IgG binding. Previously, it was demonstrated through site-directed mutagenesis that another relatively conserved change, $Ile^1 \rightarrow Ala$, in rat β_2m significantly affected IgG binding by rat FcRn (34). Another confounding variable is that there is no published information detailing the amount of β_2m expressed endogenously by MDCK cells. The possibility that canine β_2m as expressed in MDCK cells may be either deficient and/or defective with respect to human FcRn function is supported by a few anomalous observations in the only report available in this area by Praetor *et al.* (25). First, despite the ability to detect human FcRn on the cell surface by both immunofluorescence and cell surface biotinylation pH-dependent binding of IgG on the cell surface was not observed, even though FcRn in whole cell lysates retained the ability to bind IgG. Additionally, although bidirectional transcytosis of the FcRn heavy chain was demonstrated, transport of FcRn's ligand, IgG, was not described.

As a necessary prerequisite to establishing a MDCK cell model with the goal of dissecting the cell biology of human FcRn in polarized epithelia, the behavior of a constant amount of hFcRn heavy chain was compared in the absence or presence of increasing quantities of co-expressed hβ_2m. Taken together, the results indicate that hβ_2m facilitates the maturation, trafficking, and function of hFcRn in the MDCK cell line, allowing for definition in the current report of a strict hβ_2m dependence for the appropriate functional expression of hFcRn in the MDCK polarized cell model. Therefore, future structure-function studies on FcRn and, by extension, all other β_2m-dependent MHC class I-like molecules (45,46) in MDCK cells must adopt an appropriate strategy to control for this potentially confounding β_2m variable.

MATERIALS AND METHODS

Plasmid Construction and Recombinant Protein Expression

The human FcRn cDNA subcloned into pGEM7zf(+) was a kind gift of Dr. Neil Simister (Brandeis University, Waltham, MA). The cytoplasmic tail of hFcRn (residues 299 –342) was amplified from this plasmid by PCR and subcloned into the pGEX 4-T-3 vector (Amersham Biosciences, Uppsala, Sweden). Fusion proteins were purified from BL21 *Escherichia coli* as per the manufacturer's instructions.

To generate full-length hFcRn containing an NH_2-terminal HA tag (5′-YPYDVPDYA-3′), PCR was performed with a 5′ primer containing an *Eco*RI restriction site followed by the HA tag sequence fused to the first 20 base pairs of the predicted mature FcRn protein (17). The 3′ primer was specific for the COOH terminus of FcRn and included both the predicted stop translation codon and an engineered *Xho*I site. The sequences of all primers are available upon request. The PCR product was digested and subcloned into the expression vector, pcDNA3.1 (Invitrogen, Carlsbad, CA). To allow targeting into the secretory pathway, HA-FcRn was further subcloned in-frame immediately downstream of the murine MHC I K_b signal sequence, previously cloned into the pcDNA3.1 vector (referred to as pcDNAH, kind gift of Dr. Hidde Ploegh, Harvard Medical School). The entire sequence of HA-FcRn was verified by sequencing (kindly performed by Jennifer Hicks). The functionality of the MHC I k_b signal sequence in the context of FcRn was demonstrated by *in vitro* transcription and translation with and without canine microsomes (TnT Quick Coupled Transcription/Translation kit, Promega, Madison, WI). Interestingly, HA-FcRn in the context of the murine Ig_k signal sequence appeared to act anomalously in these assays as though FcRn was targeted into the secretory pathway, the Ig_k signal sequence was not cleaved (data not shown). Importantly, FcRn in the context of its endogenous signal sequence (*i.e.* FcRn cDNA) was handled normally with respect to

microsomal targeting and signal sequence cleavage. The potential effect on the cell biology of a molecule resulting from a lack of signal sequence cleavage is unclear, but was not considered in a previous study involving an NH_2-terminally FLAG-tagged human FcRn placed under the control of the same murine Ig_k signal sequence previously mentioned (25). The cDNA for human β_2m was kindly provided by Dr. Xiaoping Zhu (Brigham and Women's Hospital, Boston, MA) and subcloned into the pEF6/V5-HisA vector (Invitrogen).

Antibodies

Antibodies were raised in rabbits against the human FcRn cytoplasmic tail domain appended to glutathione *S*-transferase. Specificity of the anti-hFcRn cytoplasmic tail antisera (α-FcRnCT) was demonstrated in every protocol by the absence of a band of ~44 kDa in MDCK II cells transfected with empty parental vectors *versus* MDCK II cells transfected with the cDNA encoding human FcRn. Monoclonal antibodies 12CA5, reactive against the influenza hemagglutinin (HA) epitope, and BBM1, specific for human β_2m, were purified from hybridoma supernatants by standard methods (52). Rabbit anti-hβ_2m and anti-HA antisera, mouse anti-β-actin and anti-Golgi 58K (clone 58K-9) monoclonal antibodies (Sigma Chemical Co., St. Louis, MO), Alexa conjugated secondary antibodies (Molecular Probes, Eugene, OR), and horseradish peroxidase-conjugated secondary antibodies (Pierce, Rockford, IL) were used. The rabbit anti-endoplasmic reticulum antiserum was a generous gift of Dr. David Meyer (University of California, Los Angeles, CA).

Cells

MDCK stain II cells (kind gift of Karl Matlin, Harvard Medical School, Boston, MA) were grown in Dulbecco's modified minimal essential media (Invitrogen, Gaithersburg, MD) containing 10% fetal bovine serum (HyClone Laboratories, Logan, UT) at 37 °C, 5% CO_2. MDCK II cells were first transfected with pcDNAH.FcRn using the FuGENE reagent (Roche Molecular Biochemicals, Mannheim, Germany), selected with 0.5 mg/ml G418 (Invitrogen), and single colonies isolated using glass ring cloning cylinders. Expressing clones were identified by Western blot for the HA tag. One positive clone was then supertransfected with either pEF6/V5-HisA or pEF6.β_2m using the FuGENE reagent and selected with 8 μg/ml Blasticidin S (Invitrogen) in the continued presence of 0.5 mg/ml G418. Single colonies were screened by Western blot and immunocytochemistry. MDCK II cells transfected with the parental pcDNA3.1 and pEF6/V5-HisA vectors were additionally generated to act as negative controls. All clones were maintained with constant drug selection.

Immunocytochemistry

MDCK cells were seeded onto coverslips and grown for ~36 h at 37 °C, 5% CO_2. Following a wash with ice-cold 1× phosphate-buffered saline (PBS), the cells fixed for 20 min at 4 °C with 4% paraformaldehyde in PBS (Electron Microscopy Sciences, Ft. Washington, PA). All remaining steps were performed at room temperature in a humidified chamber. For 12CA5/rabbit anti-ER staining, fixed cells were extensively washed in 1× PBS and permeabilized with 0.2% saponin + 0.01% Triton X-100 in PBS for 20 min. For all additional primary antibody combinations, cells were permeabilized with 0.2% saponin in PBS. Nonspecific binding was blocked by incubation with 10% non-immune goat serum for 30 min (Zymed Laboratories Inc., So. San Francisco, CA). All antibody incubations were performed in the continued presence of 10% non-immune goat serum. Following extensive washing, Alexa-conjugated, species-specific goat secondary antibodies were added at a dilution of 1:400. Coverslips were mounted using the Molecular Probes Prolong Antifade reagent. All images were collected using a 60×/1.4 oil objective attached to an MRC 1024 confocal microscope (Bio-Rad). For each staining, three or four clusters of cells were analyzed by first identifying the top and bottom of the cells and then collecting serial x-y images with 0.2 μm steps. The resultant data files

were further analyzed using the tilt and rotate functions present in the Bio-Rad software, and representative sections were chosen for each clone. Final image processing and labeling was performed using Adobe Photoshop (Mountain View, CA).

Lysate Preparation, Immunoprecipitation, and Western Blotting

Depending on the assay, either confluent or subconfluent cells grown in Petri dishes were washed with ice-cold 1× PBS twice sequentially and lysis buffer supplemented with phenylmethylsulfonyl fluoride (0.17 mg/ml), leupeptin (2 μg/ml), pepstatin A (2 μg/ml), aprotinin (1 μg/ml), and bovine serum albumin (20 μg/ml), added (all protease inhibitors from Sigma). 1% Nonidet P-40 lysis buffer (50 mM Tris, pH 7.4, 150 mM NaCl, 1% Nonidet P-40, 10 mM iodoacetamide) was used for cell lysis in the pulse-chase experiments. RIPA lysis buffer (50 mM Tris, pH 7.4, 150 mM NaCl, 1% Nonidet P-40, 0.5% sodium deoxycholate, 0.1% SDS) was used for all other immunoprecipitations. Following lysis, post-nuclear supernatants were generated by centrifugation at 13,000 × *g* for 30 min at 4 °C, and lysates were quantified using the BCA assay (Pierce). Lysates were first precleared against either normal mouse serum or normal rabbit serum (both from Sigma), and antigens were recovered upon incubation with Protein A-Sepharose (Amersham Biosciences) containing prebound antibodies with gentle rotation at 4 °C overnight. Immune complexes were sequentially washed twice with lysis buffer, twice with high salt wash buffer (RIPA lysates: 50 mM Tris, pH 7.4, 500 mM NaCl, 0.1% Nonidet P-40, 0.05% sodium deoxycholate; 1% Nonidet P-40 lysates: 50 mM Tris, pH 7.4, 500 mM NaCl, 0.1% Nonidet P-40, 10 mM iodoacetamide) and once with low salt wash buffer (RIPA lysates: 50 mM Tris, pH 7.4, 0.1% Nonidet P-40, 0.05% sodium deoxycholate; 1% Nonidet P-40 lysates: 50 mM Tris, pH 7.4, 0.1% Nonidet P-40, 10 mM iodoacetamide). Proteins were resolved on 12% SDS-PAGE gels under reducing or non-reducing conditions.

Western blot analyses were performed following overnight transfer onto nitrocellulose (Schleicher and Schuell, Keene, NH). Membranes were blocked with 5% milk (Stop and Shop, Boston, MA), 0.05% Tween-20/PBS and then incubated with primary antibody with rocking for 1 h at room temperature. Following three successive washes with PBST (PBS with 0.2% Tween-20), HRP-conjugated secondary antibodies were added for 45 min, the membranes were washed three times with PBST and twice with PBS, and immunoreactive bands were visualized using the SuperSignal West Pico chemiluminescent substrate from Pierce. To reprobe a blot, membranes were incubated with stripping buffer (100 mM β-mercaptoethanol (β-ME), 2% SDS, 62.5 mM Tris, pH 6.7) at room temperature for at least 1 h and then washed extensively prior to blocking the membrane again. Quantitation of bands was performed using Quantitation One software (Bio-Rad). In brief, for each individual experiment, two or three exposures were separately quantitated and the average intensity was determined for each band in each experiment. Averages and standard deviations were calculated using such values from at least three separate experiments.

Deglycosylation Reactions

For removal of *N*-glycans from whole cell lysates, confluent 12-well dishes were lysed with 100 μl of 1% SDS and diluted to 0.5% SDS, 1% β-ME by the addition of 100 μl of 2% β-ME. The lysates were denatured at 100 °C for 10 min and then quantified using the Bradford Method (Bio-Rad). Equal quantities of lysate for each clone were then digested at 37 °C overnight in the absence (mock) or presence of either endoglycosidase H (EndoH) or peptidyl-*N*-glycanase (PNGaseF) (both from New England BioLabs). For removal of *N*-glycans post-immunoprecipitation, denaturing buffer (0.5% SDS, 1% β-ME) was added to the washed immune complexes, the precipitates were denatured at 100 °C for 10 min, and deglycosylation reactions were performed as described above.

Metabolic Labeling

MDCK cells were plated ~18 –24 h prior to metabolic labeling, at which time they were all 75–90% confluent. Cells were washed twice with prewarmed 1× PBS and then incubated in starvation medium (methionine- and cysteine-free DMEM supplemented with 10% dialyzed fetal bovine serum, Invitrogen) for 1 h at 37 °C, 5% CO_2. The starvation medium was removed, and the cells were metabolically labeled with 250 μCi/ml [^{35}S]methionine and cysteine (Easytag express protein labeling mix: PerkinElmer Life Sciences, Boston, MA) for 15 min at 37 °C, 5% CO_2. Following three washes with prewarmed 1× PBS, chase medium (DMEM with 10% fetal bovine serum supplemented with 90 μg/ml each of L-cysteine and L-methionine) was added, and the cells were incubated for the times indicated at 37 °C, 5% CO_2, at which point lysates were harvested as described above. Immunoprecipitation of metabolically labeled lysates was performed as described above except that lysates were precleared twice, instead of once, with irrelevant antibodies of the same species prior to the addition of the immunoreactive antibody (either 12CA5 or rabbit anti-hFcRnCT antisera). Densitometry was performed utilizing Quantitation One software. Data were analyzed using SigmaStat 1.0 Software (Jandel Corp., San Rafael, CA).

IgG Binding

For all experiments involving IgG binding, parallel cultures of each clone were separately lysed as described above, in either 5 mg/ml CHAPS, pH 6.0 (5 mg/ml CHAPS, 150 mM NaCl, 1 mM EDTA, 20 mM MES, pH 6.0, 10 mM iodoacetamide) or 5 mg/ml CHAPS, pH 8.0 (5 mg/ml CHAPS, 150 mM NaCl, 1 mM EDTA, 20 mM Tris, pH 8.0, 10 mM iodoacetamide). Lysates were first precleared against Protein A-Sepharose, pre-equilibrated at pH 6.0 or 8.0 for 4 h, and then incubated with IgG-Sepharose (Amersham Biosciences), pH 6.0 or 8.0, with gentle rotation at 4 °C overnight. Following three successive washes with 1 mg/ml CHAPS, pH 6.0 or 8.0, the bound fractions were either directly processed for SDS-PAGE, or alternatively, deglycosylation reactions were performed as described prior to resolution by SDS-PAGE. For experiments assessing the biochemical function of surface hFcRn, the non-binding fraction or flowthrough, following the overnight incubation with IgG-Sepharose, pH 6.0 or 8.0, was transferred into a new Eppendorf and incubated in the presence of avidin-agarose with gentle rotation at 4 °C for at least 4 h. Following extensive washing with 1 mg/ml CHAPS, pH 6.0 or 8.0, the precipitated samples were processed directly for SDS-PAGE.

Biotinylation

For all biotinylation experiments, cells were plated ~18 –24 h prior to biotinylation, at which point they were ~60 –80% confluent. Following two washes with ice-cold 1× PBS, cells were incubated with 0.5 mg/ml sulfo-NHS-biotin (Pierce) for 30 min with gentle rocking at 4 °C. This incubation was repeated with fresh sulfo-NHS-biotin. Unreacted biotin was quenched by two sequential 10-min washes with 50 mM NH_4Cl/PBS at 4 °C. Following two additional washes with ice-cold 1× PBS, cell lysates were harvested with RIPA lysis buffer as described above. For all experiments utilizing biotinylated lysates, restriction to labeling of surface molecules was confirmed by a lack of reactivity following avidin-agarose precipitation in Western blot analyses using the β-actin-specific primary antibody.

For experiments assessing the *N*-glycosylation status of surface FcRn, equal amounts of lysate for each clone were incubated in the presence of avidin-agarose (Pierce) with gentle rotation at 4 °C overnight. Following extensive washing, deglycosylation reactions on the precipitation products were performed as described above.

To detect cell surface FcRn following immunoprecipitation, nitrocellulose membranes were blocked with 0.25% gelatin blocking buffer (40 mM Trizma, pH 7.4, 5 mM EDTA, 150 mM NaCl, 0.5% Triton X-100, 0.25% fish gelatin) with rocking at 4 °C for 1 h and then incubated

with Neutravidin-HRP (Pierce, 1:10,000) diluted in gelatin blocking buffer with rocking at 4 °C for 30 min. Following three washes with PBST and two washes with PBS, reactive bands were identified as described above.

Transcytosis Assays

The ability of all MDCK clones utilized in transport assays to polarize normally was verified by the ability to preferentially incorporate [^{35}S]-Met/Cys into proteins when added to the basolateral compartment relative to the apical compartment performed essentially as described (47). For transcytosis assays, ~0.75×10^6 cells were seeded per each 12-mm diameter, 0.4-μm pore size filter (Corning Inc., Corning, NY). Transepithelial resistances were recorded daily, the cells fed on day 2 post-plating, and experiments were performed on day 3, when the measured resistances were between 150 and 200 Ωcm^2. Both surfaces were initially washed with Hanks' balanced salts containing 10 mM HEPES, pH 7.4 (HBSS+, pH 7.4), followed by a 20-min incubation at 37 °C, 5% CO_2 with 0.67% gelatin in HBSS+, pH 6.0 (HBSS with 10 mM MES, pH 6.0), on the input surface and HBSS+, pH 7.4, on the opposite, output surface. ^{125}I-Human IgG (240 nM) or ^{125}I-chicken IgY (240 nM) was then added directly to the input surface (final 60 nM for each). Cells were then incubated at 37 °C, 5% CO_2 for 2 h, at which point the entire output solution was collected, proteins were precipitated with 10% trichloroacetic acid with 2.5 μg of bovine serum albumin as a carrier, and the precipitates were counted. For blocking experiments, either 500-fold excess cold IgG or cold chicken IgY was included in the 0.67% gelatin in HBSS+, pH 6.0, and added to the input surface 20 min prior to addition of ^{125}I-IgG. Data were analyzed using SigmaStat 1.0 Software.

RESULTS

Preliminary Characterization of hFcRn Expressed in MDCK Cells in the Absence and Presence of hβ_2m

To directly assess the role of hβ_2m in hFcRn function in the MDCK cell system, a stable cell line expressing the hFcRn heavy chain was super-transfected with either a plasmid containing the cDNA for hβ_2m or the empty parental plasmid. Based upon the rationale that if hβ_2m is indeed required in some capacity for normal hFcRn function in the MDCK cell line, more hβ_2m should result in more function, four clones were selected that expressed varying quantities of hβ_2m (Fig. 1*A*, *clones* shown in *lanes 4 –7* were ranked from lowest, +, to highest, ++++, hβ_2m expression, respectively, by densitometry). To demonstrate the expression of the hFcRn heavy chain, a Western blot of whole cell lysates was performed using the monoclonal antibody, 12CA5, reactive against the NH_2-terminal HA tag appended to hFcRn (Fig. 1*B*). Interestingly, hFcRn appeared to migrate slower in the presence of co-expressed hβ_2m, suggesting that, in the presence of co-expressed hβ_2m, the single *N*-glycosylation site present in hFcRn's extracellular domain might be post-translationally modified to a different degree.

Association of hFcRn with hβ_2m was demonstrated by reciprocal co-immunoprecipitation, Western blot analyses (data not shown). Additionally, consistent with observations in neonatal rat small intestinal epithelial cells (43), hβ_2m was observed to colocalize extensively with hFcRn at steady state in all clones co-expressing hβ_2m (Fig. 1*C*, *lower merged panel*). The staining pattern for hFcRn in the absence and presence of co-expressed hβ_2m revealed a striking qualitative difference. In the absence of hβ_2m, hFcRn was confined to a predominantly perinuclear locale. Upon co-expression of hβ_2m, the majority of hFcRn was located in diffuse punctate structures throughout the cell. *Green staining* in the *merged image* of the hβ_2m co-expresser presumably represents either hFcRn complexed with canine β_2m or hFcRn that is not associated with any β_2m and likely stuck in the endoplasmic reticulum (ER). Thus, co-expression of hβ_2m alters the subcellular distribution and form of hFcRn heavy chain in MDCK cells.

Enhancement of hFcRn Maturation in the Presence of Co-expressed hβ$_2$m

To investigate the effect of hβ_2m co-expression on hFcRn heavy chain glycosylation, endoglycosidase H (EndoH) titration analyses were performed on whole cell lysates from each clone (Fig. 2*A*). EndoH cleaves the high mannose *N*-glycan moiety initially added to the consensus N*X*(S/T) sequence of nascent proteins in the ER but is unable to cleave *N*-glycans that are subsequently trimmed and modified during egress of a protein through the medial Golgi. In the absence of co-expressed hβ_2m, the majority of hFcRn contained an immature *N*-glycan as demonstrated by an increase in mobility of hFcRn following EndoH treatment (*lanes 2* and *3*). In contrast, in the presence of co-expressed hβ_2m, regardless of the quantity co-expressed, at least two distinct forms of hFcRn were detected in mock treated lysates (*lanes 4*, *7*, *10*, and *13*). When these same lysates were treated with EndoH, the slower migrating band was shown to represent hFcRn containing a mature, EndoH-resistant *N*-glycan modification whereas the faster migrating species represented hFcRn containing an immature, EndoH-sensitive *N*-glycosylation modification (*lanes 5–6*, *8 –9*, *11–12*, and *14 –15*). Additionally, there appeared to be a trend toward a higher proportion of mature, *N*-glycosylated hFcRn at steady-state levels in the context of increased hβ_2m. These studies indicate that the canine β_2m present in MDCK cells was inadequate in directing significant quantities of hFcRn maturation.

The fact that EndoH-sensitive *N*-glycosylation side-chain modifications are first attached in the ER and that a smaller percentage of the total hFcRn pool expressed in MDCK cells contained a mature, EndoH-resistant *N*-glycan in the absence *versus* the presence of co-expressed hβ_2m suggested the possibility that more hFcRn may be retained early in the secretory pathway in the hβ_2m-deficient clones. As an indirect assessment of whether hβ_2m co-expression facilitated egress of hFcRn from the ER/Golgi, the steady-state localization of hFcRn alone or in the presence of increasing amounts of hβ_2m was compared relative to the ER and Golgi. All clones expressing hFcRn revealed some colocalization with the ER (Fig. 2*B*) and Golgi (Fig. 2*C*) as expected with a stable transfectant. In the absence of co-expressed hβ_2m, the majority of the detected hFcRn overlapped with the ER (Fig. 2*B*, *top merged panel: thin arrows*), although some perinuclear staining was consistently observed that did not overlap with the ER (*arrowheads*). The possibility that this non-ER perinuclear group might represent hFcRn in the Golgi is suggested by the fact that, compared with the hβ_2m-positive clones, more overlap with a Golgi marker was observed for hFcRn in the absence of hβ_2m co-expression (Fig. 2*C*, *top merged panel: thin arrows*). In clones co-expressing hβ_2m, although some hFcRn clearly overlapped with the ER and Golgi (Fig. 2, *B* and *C*, *bottom merged panels*), there was significantly more hFcRn outside of the ER and Golgi. That hFcRn not colocalizing with either the ER or the Golgi exhibited perinuclear (*arrowheads*), diffuse punctate, and apparently cell surface (*stubby arrows*) staining patterns. These data indicate that more hFcRn achieved maturation, presumably by exiting the endoplasmic reticulum en route to the final destination of hFcRn, following proper folding in association with hβ_2m. This result also implies that canine β_2m present in MDCK cells does not associate fully with hFcRn and/or support the migration of the hFcRn heterodimer out of the ER.

Human FcRn Exhibits Faster Maturation and Increased Survival in the Presence of hβ$_2$m

Although hβ_2m clearly enhanced the ability of hFcRn to fold properly as indicated by the increased proportion of mature, *N*-glycosylated hFcRn at steady state in all clones co-expressing hβ_2m, even in clones lacking hβ_2m a minor proportion of hFcRn contained a mature EndoH-resistant *N*-glycan moiety and was therefore presumed to be properly folded in association with either endogenous canine β_2m or bovine β_2m present in the medium (Fig. 2*A* and data not shown). Focusing on the possibility that this population of mature hFcRn in the absence of hβ_2m represented a heterodimer between hFcRn and canine β_2m, the fact that only a subset of the total hFcRn pool was mature indicated that either canine β_2m was limiting

in the MDCK cell system or that canine β_2m was somehow defective with respect to the expressed hFcRn.

To compare the relative capabilities of canine and human β_2m to support hFcRn biogenesis, pulse-chase experiments were performed on two clones lacking hβ_2m and the two clones co-expressing the most hβ_2m (Fig. 3*A*). Subconfluent cultures were pulsed with [^{35}S]Met/Cys for 15 min and chased for the indicated time periods prior to lysis. Following immunoprecipitation for the hFcRn heavy chain, samples were mock treated (−) or treated (+) with EndoH (all time points), or with peptidyl *N*-glycanase F (PNGaseF, last time point only), to remove all *N*-glycans regardless of maturation. From these data (Fig. 3*A*), we first determined the fraction of mature, *N*-glycosylated hF-cRn relative to total hFcRn at each time point and calculated the rate of maturation for each clone (Fig. 3*B*). It was observed that, in the presence of hβ_2m, hFcRn acquired mature *N*-glycosylation modifications nearly 2-fold more rapidly than clones lacking hβ_2m. Furthermore, following a 4-h chase, ~88% of the hFcRn detected was mature in the presence of co-expressed hβ_2m compared with only ~50% of the hFcRn detected in the absence of co-expressed hβ_2m. Second, the percentage of hFcRn remaining 4 h post-labeling was calculated for each clone by comparing the intensities of the bands detected in the $t = 0$, EndoH-treated lanes with the $t = 240$, PNGaseF-treated lanes (Fig. 3*C*). In the presence of hβ_2m, approximately twice as much hFcRn remained 4 h post-labeling in comparison to hFcRn expressed in the absence of hβ_2m. Thus, hβ_2m expression appears to rescue hFcRn from degradation when expressed in MDCK cells.

IgG Binding Capacity of hFcRn Is Enhanced by Co-expression of hβ$_2$m

To assess IgG binding, equal quantities of CHAPS lysates pH 6.0 and 8.0, for each clone, were incubated with human IgG coupled to Sepharose beads and bound hFcRn detected by Western blot (Fig. 4*A*). As expected, hFcRn could only be detected bound to IgG at pH 6.0 (*lanes 4*, *6*, *8*, *10*, *12*, and *14*) but not pH 8.0 (*lanes 3*, *5*, *7*, *9*, *11*, and *13*), even though hFcRn was present in both the pH 6.0 and 8.0 lysates (Fig. 4*B*). More hFcRn bound IgG at pH 6.0 in lysates derived from clones co-expressing hβ_2m than in clones expressing only hFcRn. Moreover, the quantity of hβ_2m expressed and the amount of hFcRn capable of binding IgG at pH 6.0 appeared to correlate directly. Furthermore, similar to observations made in Western blots of whole cell lysates (Fig. 1*B*), increasing quantities of co-expressed hβ_2m resulted in an increased fraction of hFcRn that bound to IgG at pH 6.0 and exhibited slower migration in SDS-PAGE. Thus, increased expression of hβ_2m was associated with increased binding of hFcRn to IgG, including a fraction that exhibited migration properties suggestive of a more mature glycoprotein.

Based upon these observations, we investigated the type of post-translational modification present on the biochemically functional hFcRn in the presence and absence of co-expressed hβ_2m. IgG binding assays were performed on MDCK clones expressing hFcRn with or without hβ_2m at pH 6.0, and half of the bound proteins were either treated (+) or mock treated (*M*) with EndoH, and the other half were either treated (+) or mock treated (*M*) with PNGaseF (Fig. 5). In the absence of co-expressed hβ_2m, the majority of hFcRn capable of binding IgG contained an immature *N*-glycan moiety (*lanes 2–3* and *6–7*). In contrast, co-expressed hβ_2m significantly increased the proportion of EndoH-resistant, mature hFcRn capable of binding IgG at pH 6.0, although some EndoH-sensitive hFcRn was still detectable (*lanes 11* and *15*). There thus appeared to be a direct correlation between the amount of hβ_2m expressed and not only the quantity of hFcRn capable of binding IgG but also the proportion of EndoH-resistant, mature *N*-glycosylated hFcRn detected in this biochemically functional fraction.

Co-expression of hβ$_2$m Increases Localization of Biochemically Functional and Mature hFcRn to the Cell Surface

We next examined the impact of hβ_2m co-expression on the surface expression of the hFcRn heavy chain at steady state. Following cell surface biotinylation, hFcRn was immunoprecipitated from a control MDCK clone (Fig. 6*A*, *lane 1*), two clones expressing hFcRn alone (*lanes 2* and *3*), and two clones co-expressing the most hβ_2m (*lane 4*, +++; *lane 5*, ++++). Whether hFcRn was immunoprecipitated with the monoclonal antibody, 12CA5, or a rabbit anti-hFcRn cytoplasmic tail antiserum, there was a marked increase in the amount of hFcRn present on the cell surface in the presence of co-expressed hβ_2m *versus* its absence, even though equivalent quantities of hFcRn were immunoprecipitated from each clone (Fig. 6*B*). Importantly, no ~44-kDa band could be detected in lysates derived from control MDCK transfectants (Fig. 6, *A* and *B*, *lanes 1*). A band of ~12 kDa present on the surface (Fig. 6*A*, *lanes 4* and *5*) was co-immunoprecipitated with hFcRn and subsequently demonstrated to consist primarily of hβ_2m (Fig. 6*C*). It is worth noting that, upon longer exposure, a faint ~12-kDa band, which co-immunoprecipitated with hFcRn, could be detected on the surface in clones expressing hFcRn alone and presumably represents either canine or bovine β_2m (data not shown).

As hβ_2m increased both the ability of hFcRn to mature and reach the cell surface, the *N*-glycosylation status of surface hFcRn was examined. Following biotinylation, surface proteins were precipitated with avidin-agarose, and half of the bound proteins was treated (+) or mock treated (*M*) with EndoH and the other half treated (+) or mock treated with PNGaseF prior to Western blotting for hFcRn (Fig. 7). Consistent with the previous results (Fig. 6), significantly more hFcRn could be detected on the cell surface in the presence of co-expressed hβ_2m than when hFcRn was expressed alone. Regardless of hβ_2m co-expression, all cell surface hFcRn contained a mature, EndoH-resistant *N*-glycan moiety (Fig. 7, *lanes 3*, *7*, *11*, and *15*).

To further ascertain the biochemical functionality of surface hFcRn, parallel subconfluent dishes were surface-biotinylated, lysed in CHAPS lysis buffer at either pH 6.0 or 8.0, and IgG binding assays were performed. The flow-through following IgG binding was then incubated with avidin-agarose, to precipitate surface proteins, prior to Western blotting for hFcRn (Fig. 8*A*). In this assay, the biochemical functionality of surface hFcRn is demonstrated by the ability to only detect hFcRn following IgG binding at pH 8.0 but not pH 6.0. This pattern was in fact observed for both clones co-expressing hβ_2m. In the presence of hβ_2m, the vast majority of surface hFcRn was capable of binding IgG in a pH-dependent manner. Residual surface hFcRn could be detected following IgG binding at pH 6.0 (*lanes 8* and *10*), presumably reflecting saturation of the IgG-Sepharose beads in the experiment shown. In the absence of co-expressed hβ_2m, small quantities of functional hFcRn could be identified on the cell surface (*lane 3*) further indicating the inability of canine β_2m to provide adequate functionality to exogenously expressed hFcRn in the MDCK cell line. Taken together, these data demonstrate that hβ_2m allows much more hFcRn to reach the cell surface and that this cell surface hFcRn is both mature, as defined by its *N*-glycosylation pattern, and active with respect to its ability to bind IgG.

Increased Bidirectional Transport of IgG in the Presence of Co-expressed Hβ$_2$m

FcRn-dependent bidirectional transport of IgG has been reported in several polarized cell models (22–26). We therefore tested the relative ability of hFcRn to transcytose ^{125}I-labeled IgG in both the apical to basolateral and basolateral to apical directions with and without co-expressed hβ_2m (Fig. 9, *A* and *B*, respectively). Specificity for FcRn-dependent IgG transport was directly tested by the ability to block transport with cold human IgG but not cold chicken IgY, which is unable to bind FcRn. Nonspecific transport for each clone was further examined using ^{125}I-labeled IgY as a probe. For basolateral to apical transport, every MDCK cell line

that expressed hFcRn, regardless of hβ_2m co-expression, exhibited FcRn-mediated transcytosis of ^{125}I-IgG as demonstrated by the ability to block the transport of ^{125}I-IgG with excess cold human IgG but not chicken IgY (Fig. 9*B*). Calculation of FcRn-specific transport revealed that all clones examined exhibited significant transport of IgG relative to the control MDCK cell line. Importantly, co-expression of hβ_2m increased the basolateral to apical transport of IgG relative to the transport observed in clones expressing the hFcRn heavy chain alone.

In contrast to the transcytosis of IgG in the basolateral to apical direction, only one of the three clones expressing hFcRn alone exhibited FcRn-mediated transport of IgG in the apical to basolateral direction (Fig. 9*A*). When the FcRn-specific transport was calculated for this direction, the MDCK clones expressing hFcRn alone as a group exhibited insignificant transport of IgG relative to the control MDCK cell line. In contrast, co-expression of hβ_2m with hFcRn increased FcRn-specific transport of ^{125}I-IgG to significant levels beyond that observed in both control MDCK cell lines and clones expressing the hFcRn heavy chain alone. In the apical to basolateral direction, there was some apparent dampening effect of the underivatized chicken IgY on the transport of ^{125}I-IgG. Although the reason for this effect is both unexpected and not understood, the fact that the transport of ^{125}I-IgG was significantly different between the IgG and IgY block experiments where indicated underscores the important contribution of hFcRn in this transport. Taken together, these data indicate that hβ_2m co-expression increases the bidirectional transport of IgG by hFcRn in MDCK cells.

DISCUSSION

In the present study, we demonstrate by a direct comparison of clones expressing a relatively constant level of human FcRn heavy chain alone or in the presence of varying quantities of hβ_2m, the importance of co-expressing the homologous hβ_2m subunit in reconstituting hFcRn function in MDCK cells. When the only potential sources of β_2m were species-mismatched (either endogenous canine β_2m or bovine β_2m in serum), hFcRn was impaired in its ability to acquire mature, EndoH-resistant *N*-glycosylation modifications and thus presumably to fold correctly, mature with a rapid kinetics, bind IgG, and reach the cell surface. Most importantly, hβ_2m co-expression not only increased the transport of IgG across polarized MDCK monolayers but was in fact required for significant FcRn-specific transport of IgG in the apical to basolateral direction. We conclude that hβ_2m is required to obtain full hFcRn function in the MDCK cell system. As such, future molecular dissection of hFcRn and, by extension, likely all MHC I-related molecules in MDCK cells must utilize a strategy in which hβ_2m expression levels are normalized between heavy chain mutants.

One limitation of this work is that, although the impact of hβ_2m on hFcRn expression and function in MDCK cells is clearly demonstrated, the exact reason for the need for this expression remains unclear. The bulk of these data is entirely consistent with a low expression level of endogenous canine β_2m by MDCK cells. In this scenario, it is the simple expression of more β_2m that is the cause for the observed effects of hβ_2m on hFcRn. However, the combined results of the pulse-chase experiments (Fig. 3) suggest that canine β_2m does not efficiently support the biogenesis of the hFcRn heavy chain. If canine β_2m is simply limiting, co-expression of hβ_2m would be predicted to rescue a proportion of newly synthesized hFcRn from degradation. There should, however, be no effect on the kinetics of maturation for that population of rescued hFcRn. However, the kinetics of hFcRn maturation was significantly increased in the presence of hβ_2m, arguing that canine β_2m is partially defective in its ability to facilitate hFcRn biogenesis. The fact that a ~12-kDa band was co-immunoprecipitated with hFcRn from clones expressing hFcRn alone may indicate that this proposed defect doesn't involve a complete inability to associate with hFcRn. Furthermore, the presence of this co-immunoprecipitated, ~12-kDa band provides evidence that endogenous canine β_2m can be readily radiolabeled and therefore might not be limiting. This proposed defect associated with

canine β_2m does not completely abolish IgG binding, although potential quantitative differences in the binding affinity of hFcRn in association with canine *versus* human β_2m for IgG were not determined. Although much more hFcRn accessed the cell surface in the presence of hβ_2m, the fact that the *N*-glycosylation profile of surface hFcRn was mature regardless of co-expressed hβ_2m argues that the pathway taken to the surface was at least similar, if not the same. Our work also provides a rationale for previously unexplained observations made by Praetor *et al.* (25). Consistent with their work involving hFcRn expressed alone in MDCK cells, we show here that cell surface-biotinylated hFcRn solubilized in CHAPS lysis buffer cannot be convincingly demonstrated to bind IgG in the absence of co-expressed hβ_2m (Fig. 8), even though hFcRn solubilized from whole cell lysates does retain some IgG binding capacity (Fig. 4). This may be due to the fact that, in the absence of hβ_2m, only small amounts of hFcRn reach the cell surface and/or reflect a quantitative difference in the IgG binding affinity of an hFcRn/canine β_2m heterodimer. Unfortunately, but entirely consistent with another study on hFcRn (48), we (data not shown) have been unable to demonstrate FcRn-specific binding of IgG at 4 °C with intact cells. Thus, it is difficult to directly assess the relative binding affinities of the hFcRn/hβ_2m and hFcRn/canine β_2m heterodimers in these cell lines.

Similar to rat FcRn expressed in IMCD cells (26,39,40), multiple *N*-glycosylated forms are observed when hFcRn is expressed with hβ_2m in MDCK cells. In both circumstances, the slower migrating forms represent FcRn containing one or more mature *N*-glycans, whereas the faster migrating band consists of FcRn containing one or more EndoH-sensitive *N*-glycan moieties. Notably, rat FcRn contains four potential *N*-glycosylation sites, whereas human FcRn contains only a single consensus *N*-glycosylation motif. In stark contrast to rat FcRn expressed in IMCD cells, in which apparently immature FcRn could be demonstrated on the cell surface (39), only mature *N*-glycosylated hFcRn could be detected on the surface of MDCK cells as described here. This would seem to argue that, for hFcRn expressed in MDCK cells, a conventional route is traveled by hFcRn on the way to the cell surface, with the modifications resulting in EndoH resistance for hFcRn's single *N*-glycan occurring as it passes through the Golgi out to the cell surface. Alternatively, hFcRn could travel from the ER directly to the cell surface, as has been proposed for rat FcRn in IMCD cells (39). In this scenario, the reason we could detect no immature *N*-glycosylated hFcRn on the surface would presumably reflect a very rapid re-internalization and subsequent trafficking into the *cis*-medial Golgi, where the high mannose *N*-glycan is trimmed and modified. It was previously speculated (39) that this itinerary would allow rat FcRn on the surface to re-internalize unbound to IgG, due to the importance of a proposed carbohydrate handshake in the formation of a high affinity FcRn dimer (49). Thus, in this case, IgG binding would be conferred only when rat FcRn had trafficked retrograde into the *Cis*-medial Golgi and its *N*-glycans trimmed and processed. One problem with this model is that both rat and mouse FcRn containing only immature *N*-glycan modifications have been demonstrated to bind IgG (36,50), demonstrating that mature *N*-glycan modifications on FcRn are not required to form a high affinity interaction with IgG. Consistent with this observation for rodent FcRn, we demonstrate that hFcRn containing immature *N*-glycans can bind IgG in a pH-dependent manner. Taken together with the observation that only mature, *N*-glycosylated hFcRn could be detected on the cell surface suggests that hFcRn acquires the ability to bind IgG prior to reaching the cell surface. Given that immature hFcRn could bind IgG but only mature *N*-glycosylated hFcRn could be detected on the cell surface of MDCK cells, we favor the model in which newly synthesized hFcRn associates rapidly with hβ_2m and, once having passed the ER quality control machinery, follows the normal secretory pathway en route to its final destination, which at least in part includes the cell surface plasma membrane. In this situation, the fact that FcRn (43) but not internalized IgG (15) could be detected in the Golgi cisternae of neonatal rat intestinal epithelial cells may simply reflect the fact that FcRn doesn't traffic through the Golgi post-biosynthesis or, alternatively, that the transcytotic pathway taken by rat FcRn bound to IgG in the apical to basolateral direction does not include the Golgi as part of its itinerary.

One other potential explanation for the presence of EndoH-sensitive hFcRn capable of binding IgG at pH 6.0 in all clones regardless of co-expressed hβ_2m (Fig. 5) is that this represents hFcRn in association with canine β_2m. If true, the presence of EndoH-sensitive hFcRn in all clones regardless of hβ_2m expression could simply reflect the proposed defect in canine β_2m with respect to hFcRn's biogenesis. If so, this biochemically functional mixed species heterodimer is likely retained within the ER, as we demonstrated above, and thus immature with respect to hFcRn's *N*-glycosylation modification.

Previous work on human FcRn in MDCK cells failed to consider the possible importance of β_2m in this system (25). Our present work therefore allows for some additional interpretations. Like the clones expressing hFcRn alone in our present study, the FLAG-tagged FcRn in the previous work (25) exhibited a perinuclear staining pattern that we now show is largely due to expression within the ER/Golgi. In the absence of hβ_2m, both works also demonstrated that IgG binding was grossly intact and that only low levels of hFcRn could reach the cell surface. Therefore, in the context of our present work, we can likely predict that Praetor *et al.* (24,25) were largely evaluating an immature population of hFcRn that retained the ability to bind IgG. Whether the presence of a retained, un-cleaved signal sequence, which we have also demonstrated as likely to be the case for the hFcRn protein expressed by Praetor and colleagues, further contributed to this immature population of hFcRn is unclear (see "Materials and Methods"). One notable difference is that, although the previous work of Praetor *et al.* demonstrated bidirectional transcytosis of the receptor alone, our present work has revealed significant transport of IgG, FcRn's ligand, only in the basolateral to apical direction in the absence of co-expressed hβ_2m. Only in the presence of co-expressed hβ_2m was any significant transport of IgG in the apical to basolateral direction demonstrated. Even though FcRn-mediated transcytosis in the basolateral to apical direction was observed in MDCK cells expressing hFcRn alone, the presence of co-expressed hβ_2m significantly increased transport of IgG by hFcRn in this direction. Whether the observed dependence on hβ_2m co-expression for transport in the apical to basolateral direction represents a specific defect of a mixed species hFcRn/canine β_2m heterodimer or, alternatively, simply reflects a limitation in detection is unclear. Whether the observed differences in transcytotic capacity simply reflect the amount of hFcRn available at each cell surface or are the result of fundamental differences in the two pathways is currently unknown and will be addressed in MDCK cells stably transfected with hβ_2m and then supertransfected with hFcRn. A detailed analysis of hFcRn cell biology in this context is now deemed most appropriate, because it will essentially negate the hβ_2m variable extant in the current cell lines and allow direct comparison of the trafficking properties of full-length hFcRn *versus* assorted FcRn heavy chain mutants.

Interestingly, the increased capacity to transport IgG in the basolateral to apical direction *versus* the apical to basolateral direction by hFcRn as expressed by MDCK cells is essentially the reverse of what has been reported for rat FcRn either expressed alone in the rat IMCD cell line (26) or together with the rat β_2m in MDCK cells (51). In the recent report by Ramalingam *et al.* (51), it was observed that exposure of MDCK cells expressing rat FcRn to either rat or bovine IgG caused an apical to basolateral redistribution of rat FcRn. Based on the fact that, following a 1-h serum starvation, the majority of rat FcRn localized apically in polarized MDCK cells, it was suggested that a plausible explanation for the 80:20 basolateral to apical steady-state distribution observed for rat FcRn on filter-grown IMCD cells (39) was that their assay was performed without a serum starvation prior to adding probe. Despite this lack of serum starvation in either the Fc binding assays or transcytosis assays performed by Simister and colleagues, 2-fold greater FcRn-dependent transport of IgG in the apical to basolateral direction relative to the basolateral to apical direction was observed. When serum starvation was performed, the kinetics of IgG transport was noted to be initially more rapid in both directions (26). Moreover, the total cumulative quantity of transported IgG in the apical to basolateral direction was increased 5-fold relative to both transport in the same direction

without serum starvation, and perhaps more tellingly, in the basolateral to apical direction with prior serum starvation. Given that more FcRn-dependent transport of IgG was observed in the basolateral to apical direction compared with the apical to basolateral direction following a 40-min serum starvation (compared with the 60-min serum starvation performed for rat FcRn in MDCK cells), as demonstrated in the present study, strongly suggests that rat and human FcRn have different transcytotic propensities, if not itineraries. Whether the disparate transcytotic abilities reflect fundamental differences in the biology of rat *versus* human FcRn, such as the need to transport IgG across the small intestine *versus* the placenta, or are simply a byproduct of subtle differences in the two species' receptors, such as the number of *N*-glycan moieties attached, is currently an interesting and open question.

Acknowledgments

S. M. C. thanks Drs. Karl Matlin, Hidde Ploegh, and Cox Terhorst for critically important guidance and thoughtful discussions, Dr. Susan Hagen for help with confocal microscopy, and Drs. K. Badizadigan and F. E. Johansen for critical review of the manuscript.

References

1. Mostov KE, Deitcher DL. Cell 1986;46:613–621. [PubMed: 3524859]
2. Apodaca G, Katz LA, Mostov KE. J Cell Biol 1994;125:67–86. [PubMed: 8138576]
3. Luton F, Verges M, Vaerman JP, Sudol M, Mostov KE. Mol Cell 1999;4:627–632. [PubMed: 10549294]
4. Leung SM, Rojas R, Maples C, Flynn C, Ruiz WG, Jou TS, Apodaca G. Mol Biol Cell 1999;10:4369–4384. [PubMed: 10588664]
5. Brown PS, Wang E, Aroeti B, Chapin SJ, Mostov KE, Dunn KW. Traffic 2000;1:124–140. [PubMed: 11208093]
6. Wang E, Brown PS, Aroeti B, Chapin SJ, Mostov KE, Dunn KW. Traffic 2000;1:480–493. [PubMed: 11208134]
7. Rodewald R. J Cell Biol 1976;71:666–669. [PubMed: 11223]
8. Abrahamson DR, Rodewald R. J Cell Biol 1981;91:270–280. [PubMed: 7298722]
9. Brambell FW. Lancet 1966;2:1087–1093. [PubMed: 4162525]
10. Ghetie V, Hubbard JG, Kim JK, Tsen MF, Lee Y, Ward ES. Eur J Immunol 1996;26:690–696. [PubMed: 8605939]
11. Israel EJ, Wilsker DF, Hayes KC, Schoenfeld D, Simister NE. Immunology 1996;89:573–578. [PubMed: 9014824]
12. Junghans RP, Anderson CL. Proc Natl Acad Sci U S A 1996;93:5512–5516. [PubMed: 8643606]
13. Christianson GJ, Brooks W, Vekasi S, Manolfi EA, Niles J, Roopenian SL, Roths JB, Rothlein R, Roopenian DC. J Immunol 1997;159:4781–4792. [PubMed: 9366402]
14. Jones E, Waldmann T. J Clin Invest 1972;51:2916–2927. [PubMed: 5080417]
15. Rodewald R. J Cell Biol 1973;58:189–211. [PubMed: 4726306]
16. Israel EJ, Patel VK, Taylor SF, Marshak-Rothstein A, Simister NE. J Immunol 1995;154:6246–6251. [PubMed: 7759862]
17. Story CM, Mikulska JE, Simister NE. J Exp Med 1994;180:2377–2381. [PubMed: 7964511]
18. Simister NE, Story CM, Chen HL, Hunt JS. Eur J Immunol 1996;26:1527–1531. [PubMed: 8766556]
19. Kristoffersen EK. APMIS Suppl 1996;64:5–36. [PubMed: 8944053]
20. Antohe F, Radulescu L, Gafencu A, Ghetie V, Simionescu M. Hum Immunol 2001;62:93–105. [PubMed: 11182218]
21. Firan M, Bawdon R, Radu C, Ober RJ, Eaken D, Antohe F, Ghetie V, Ward ES. Int Immunol 2001;13:993–1002. [PubMed: 11470769]
22. Dickinson BL, Badizadegan K, Wu Z, Ahouse JC, Zhu X, Simister NE, Blumberg RS, Lencer WI. J Clin Invest 1999;104:903–911. [PubMed: 10510331]

23. Ellinger I, Schwab M, Stefanescu A, Hunziker W, Fuchs R. Eur J Immunol 1999;29:733–744. [PubMed: 10092075]
24. Stefaner I, Praetor A, Hunziker W. J Biol Chem 1999;274:8998 –9005. [PubMed: 10085147]
25. Praetor A, Ellinger I, Hunziker W. J Cell Sci 1999;112:2291–2299. [PubMed: 10381385]
26. McCarthy KM, Yoong Y, Simister NE. J Cell Sci 2000;113:1277–1285. [PubMed: 10704378]
27. Huber AH, Kelley RF, Gastinel LN, Bjorkman PJ. J Mol Biol 1993;230:1077–1083. [PubMed: 8478919]
28. Burmeister WP, Huber AH, Bjorkman PJ. Nature 1994;372:379 –383. [PubMed: 7969498]
29. Kim JK, Tsen MF, Ghetie V, Ward ES. Eur J Immunol 1994;24:2429 –2434. [PubMed: 7925571]
30. Kim JK, Tsen MF, Ghetie V, Ward ES. Eur J Immunol 1994;24:542–548. [PubMed: 8125126]
31. Raghavan M, Chen MY, Gastinel LN, Bjorkman PJ. Immunity 1994;1:303–315. [PubMed: 7889418]
32. Raghavan M, Wang Y, Bjorkman PJ. Proc Natl Acad Sci U S A 1995;92:11200 –11204. [PubMed: 7479965]
33. Popov S, Hubbard JG, Kim J, Ober B, Ghetie V, Ward ES. Mol Immunol 1996;33:521–530. [PubMed: 8700168]
34. Vaughn DE, Milburn CM, Penny DM, Martin WL, Johnson JL, Bjorkman PJ. J Mol Biol 1997;274:597–607. [PubMed: 9417938]
35. Vaughn DE, Bjorkman PJ. Biochemistry 1997;36:9374 –9380. [PubMed: 9235980]
36. Sanchez LM, Penny DM, Bjorkman PJ. Biochemistry 1999;38:9471–9476. [PubMed: 10413524]
37. West AP Jr, Bjorkman PJ. Biochemistry 2000;39:9698 –9708. [PubMed: 10933786]
38. Kobayashi N, Suzuki Y, Tsuge T, Okumura K, Ra C, Tomino Y. Am J Physiol 2002;282:F358 –F365.
39. Wu Z, Simister NE. J Biol Chem 2001;276:5240 –5247. [PubMed: 11096078]
40. McCarthy KM, Lam M, Subramanian L, Shakya R, Wu Z, Newton EE, Simister NE. J Cell Sci 2001;114:1591–1598. [PubMed: 11282034]
41. Simister NE, Rees AR. Eur J Immunol 1985;15:733–738. [PubMed: 2988974]
42. Simister NE, Mostov KE. Nature 1989;337:184 –187. [PubMed: 2911353]
43. Berryman M, Rodewald R. J Cell Sci 1995;108:2347–2360. [PubMed: 7673354]
44. Smithies O, Poulik M. Proc Natl Acad Sci U S A 1972;69:2914–2917. [PubMed: 4507614]
45. Rodionov DG, Nordeng TW, Pedersen K, Balk SP, Bakke O. J Immunol 1999;162:1488 –1495. [PubMed: 9973405]
46. Rodionov DG, Nordeng TW, Kongsvik TL, Bakke O. J Biol Chem 2000;275:8279 –8282. [PubMed: 10722655]
47. Balcarova-Stander J, Pfeiffer SE, Fuller SD, Simons K. EMBO J 1984;3:2687–2694. [PubMed: 6391916]
48. Ober RJ, Radu CG, Ghetie V, Ward ES. Int Immunol 2001;13:1551–1559. [PubMed: 11717196]
49. Vaughn DE, Bjorkman PJ. Structure 1998;6:63–73. [PubMed: 9493268]
50. Martin WL, Bjorkman PJ. Biochemistry 1999;38:12639 –12647. [PubMed: 10504233]
51. Ramalingam TS, Detmer SA, Martin WL, Bjorkman PJ. EMBO J 2002;21:590 –601. [PubMed: 11847107]
52. Harlow, E.; Lane, D. Antibodies: A Laboratory Manual. Cold Spring Harbor Laboratory; Cold Spring Harbor, NY: 1988.

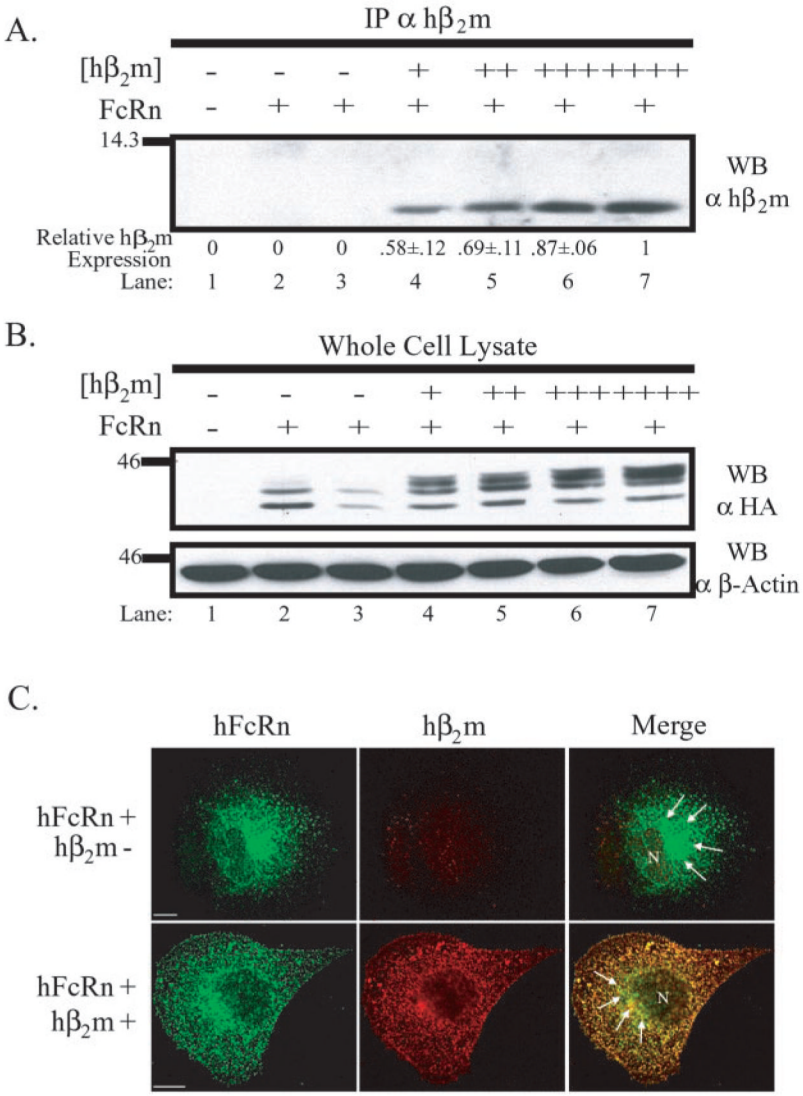

Fig. 1. hβ_2m alters the migration of hFcRn by SDS-PAGE and steady-state distribution

A, hβ_2m immunoprecipitates of indicated lysates were resolved by SDS-PAGE under non-reducing conditions, and a Western blot analysis was performed using a rabbit anti-hβ_2m antiserum. Following quantitation, the ratio of hβ_2m expressed per clone relative to the clone with the highest expression was calculated (mean ± S.E. n = 5). Lysates were from MDCK II cells transfected with: (i) both empty vectors (*lane 1*), (ii) FLFcRn$^{\#1}$ and pEF6/V5-HisA (*lanes 2* and *3*), or (iii) FLFcRn$^{\#1}$ and pEF6.hβ_2m (*lanes 4 –7*). *B*, 50 μg of RIPA lysate from the same MDCK II transfectants as in *A* were separated by 12% SDS-PAGE under reducing conditions, and a Western blot analysis for hFcRn was performed using the monoclonal antibody 12CA5 (*α HA*). The *bottom panel* is the same membrane reprobed for *β*-actin to demonstrate equal loading. The *images* are the results of one representative experiment (n = 3). The molecular mass in kilodaltons is shown on *left*. *C*, MDCK clones expressing a constant amount of hFcRn in the absence or presence of co-expressed hβ_2m (as previously defined and indicated at *left*) were doubled-stained with a rabbit anti-HA antiserum (*green column*) and BBM1 (*red column*), which is specific for human β_2m. Specific staining was revealed using species-specific, Alexa-conjugated secondary antibodies. Analysis was performed by confocal microscopy. The *third column* in each *row* shows *merged images*. Control MDCK cells

revealed no specific staining with either primary antibody (data not shown). *Arrows* highlight intense perinuclear staining, which is common to both hβ_2m-negative and -positive clones.hβ_2m-positive clones additionally displayed diffuse, punctate staining. *N* specifies the location of the nucleus. *Bars* = 10 μm.

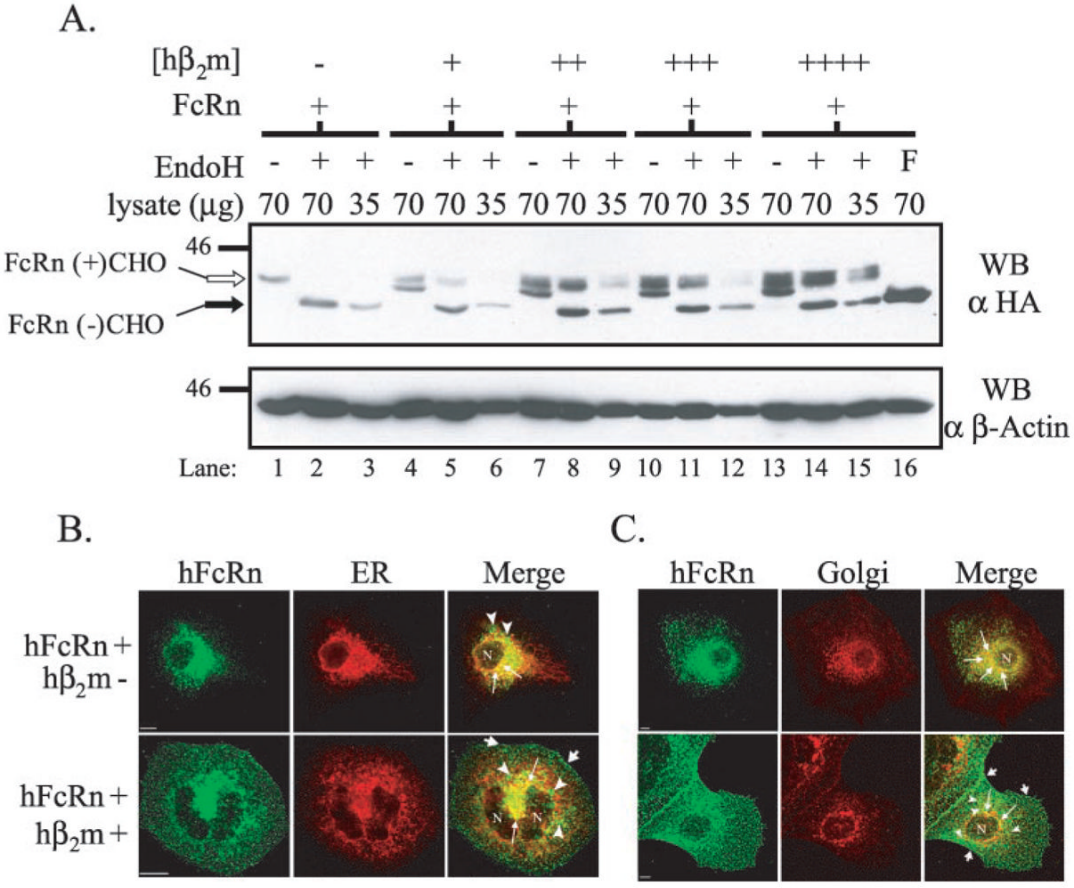

Fig. 2. hβ_2m both increases the fraction of mature, *N*-glycosylated FcRn and decreases the proportion of FcRn resident to the ER/Golgi at steady-state

A, confluent plate-grown cells were lysed, and deglycosylation reactions were performed. Reaction conditions were: mock (−), EndoH (+), and PNGaseF (*F*). Reaction products from the quantity (micrograms) of lysate indicated were analyzed by SDS-PAGE and Western blotting for the HA tag as previously described. The *bottom panel* is the same membrane reprobed for *β*-actin. Samples were as follows: *lanes 1–3*, FLFcRn$^{\#1}$ and pEF6/V5-HisA; *lanes 4 –6*, FLFcRn$^{\#1}$ and pEF6.hβ_2m (low: +); *lanes 7–9*, FLFcRn$^{\#1}$ and pEF6.hβ_2m (mid: ++); *lanes10–12*, FLFcRn$^{\#1}$ and pEF6.hβ_2m (mid/high: +++); and *lanes 13–16*, FLFcRn$^{\#1}$ and pEF6.hβ_2m (high: ++++) where the relative amount of expressed hβ_2m is denoted in *parentheses*. The *bands* corresponding to glycosylated FcRn (*FcRn+CHO: open arrow*) and deglycosylated FcRn (*FcRn-CHO: black arrow*) are labeled (n = 5). *B* and *C*, MDCK clones expressing a constant amount of hFcRn in the absence or presence of co-expressed hβ_2m (as previously defined and indicated at *left*) were doubled-stained for FcRn (*green column*) and either the ER (*B*, *red column*) or Golgi (*C*, *red column*). Specific staining was revealed using species-specific, Alexa-conjugated secondary antibodies. Analysis was performed by confocal microscopy. The *third column* in each *row* shows *merged images. N* specifies the location of the nucleus. *Bars* = 10 μm.

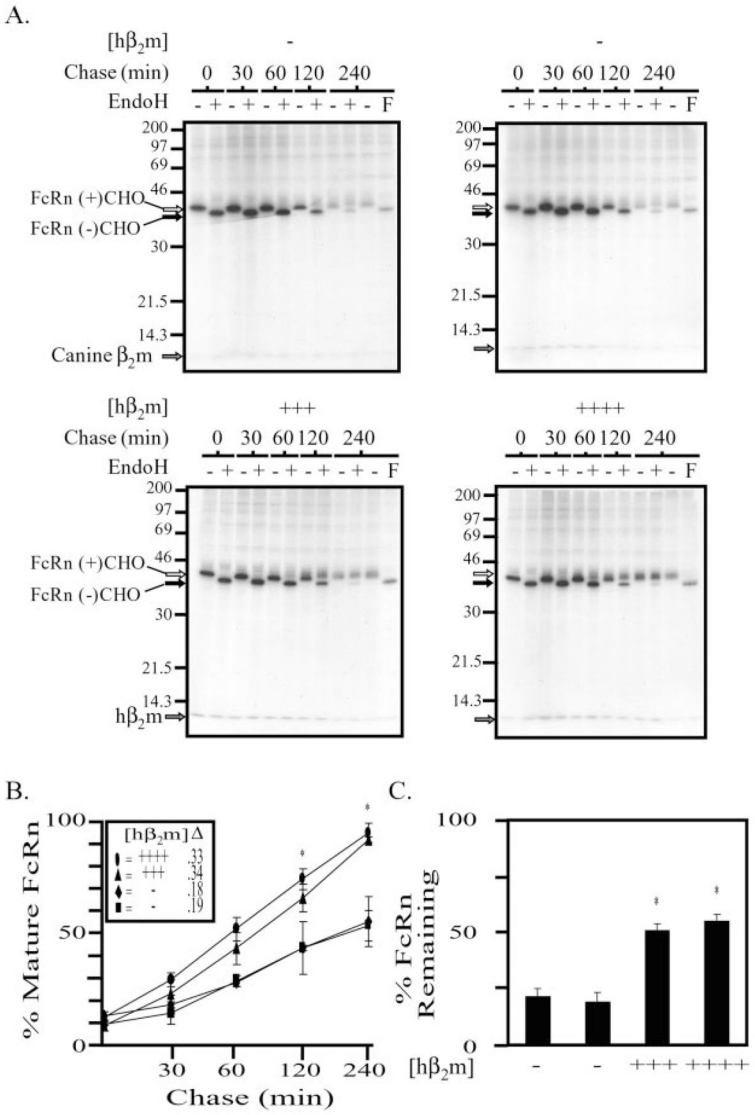

Fig. 3. FcRn matures with a faster kinetics, and more newly synthesized FcRn survives to maturity in the presence *versus* the absence of co-expressed hβ_2m

A, MDCK clones expressing hFcRn alone (*top*) or in the presence of increasing amounts of co-expressed hβ_2m (*bottom*) were pulse-labeled for 15 min with [^{35}S]methionine/cysteine and chased at 37 °C, 5% CO_2. At the indicated times, cells were lysed in 1% Nonidet P-40 lysis buffer, and immunoprecipitations were performed using rabbit anti-FcRnCT antiserum. The immunoprecipitation products were divided and treated (+) or mock treated (−) with EndoH as previously described prior to analysis by SDS-PAGE and autoradiography. An additional 240-min chase was performed, and following immunoprecipitation for hFcRn, treated (*F*) or mock treated (−) with PNGaseF. The position of a very faint band of ~12 kDa, which co-immunoprecipitates with hFcRn in both clones not co-expressing hβ_2m, is indicated with a *gray arrow* and is presumed to be canine β_2m. A more intense ~12-kDa band is co-immunoprecipitated with hFcRn in both clones co-expressing hβ_2m (*gray arrow* on *two lower gels*). Glycosylated hFcRn (*open arrow*) and deglycosylated hFcRn (*black arrow*) are indicated. The migration of molecular mass markers is indicated at the *left* of all gels. The exposure time for all four gels was 23 h. *B* and *C*, data from three separate experiments were

quantitated using Quantitation One software (Bio-Rad). *B*, the percent mature FcRn was calculated for each time point as follows: $R/(R + S) \times 100$, where *R* is the volume of EndoH^{res} FcRn and *S* is the volume of EndoH^{sens} FcRn. The rate of maturation, defined by the resultant slope (Δ), was calculated for each clone and is provided next to the appropriate symbol in the *inset*. ANOVA $p = 0.001$. The *asterisk* indicates statistical significance relative to the MDCK clones expressing only the hFcRn heavy chain (hFcRn+/hβ_2m−) at $p \leq 0.05$ by multiple comparison procedures. *C*, the percent FcRn surviving after a 4-h chase was calculated as follows: $X/Y \times 100$, where *X* is the volume of FcRn in the PNGaseF-treated 240-min time point and *Y* is the volume of FcRn in EndoH-treated 0-min time point. ANOVA $p = 0.000002$. The *asterisk* indicates statistical significance relative to the MDCK clones expressing only the hFcRn heavy chain (hFcRn+/hβ_2m−) at $p \leq 0.05$ by multiple comparison procedures (mean ± S.E. $n = 3$).

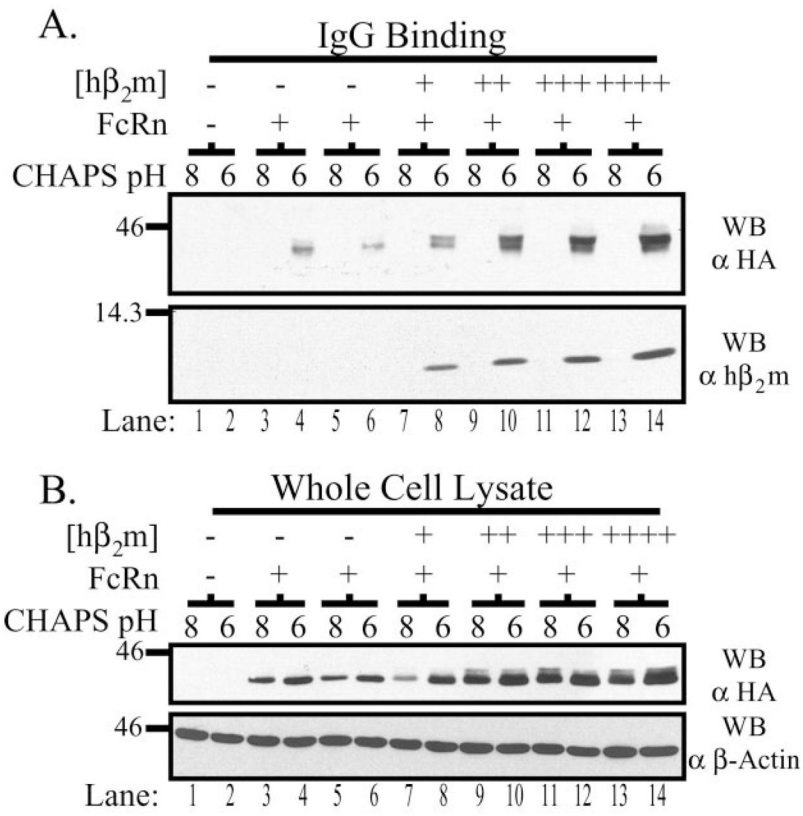

Fig. 4. hβ_2m expression levels correlate directly with IgG binding capacity

A, confluent monolayers were harvested in 5 mg/ml CHAPS lysis buffer, pH 6.0 or 8.0, and 500 μg of precleared lysate was incubated with IgG-Sepharose beads rotating gently at 4 °C overnight. Bound proteins were analyzed by SDS-PAGE under non-reducing conditions and Western blotting for the HA tag and hβ_2m as previously described. Samples are as follows: *lanes 1–2*, both empty vectors; *lanes 3–4* and *5–6*, FLFcRn$^{\#1}$ and pEF6/V5-HisA (two different clones); *lanes 7–8*, FLFcRn$^{\#1}$ and pEF6.hβ_2m (low:+); *lanes 9–10*, FLFcRn$^{\#1}$ and pEF6.hβ_2m (mid: ++); *lanes 11–12*, FLFcRn$^{\#1}$ and pEF6.hβ_2m (mid/high: +++); and *lanes 13–14*, FLFcRn$^{\#1}$ and pEF6.hβ_2m (high: ++++) where the relative amount of expressed hβ_2m is denoted in *brackets*. *B*, 30 μg of each lysate was directly analyzed by Western blot for the HA tag to verify that FcRn was solubilized at pH 6.0 and 8.0 (*top gel*). This blot was then stripped and reprobed for β-actin. The *images* are the results of one representative experiment (n = 7). The molecular mass in kilodaltons is indicated on the *left* of each gel.

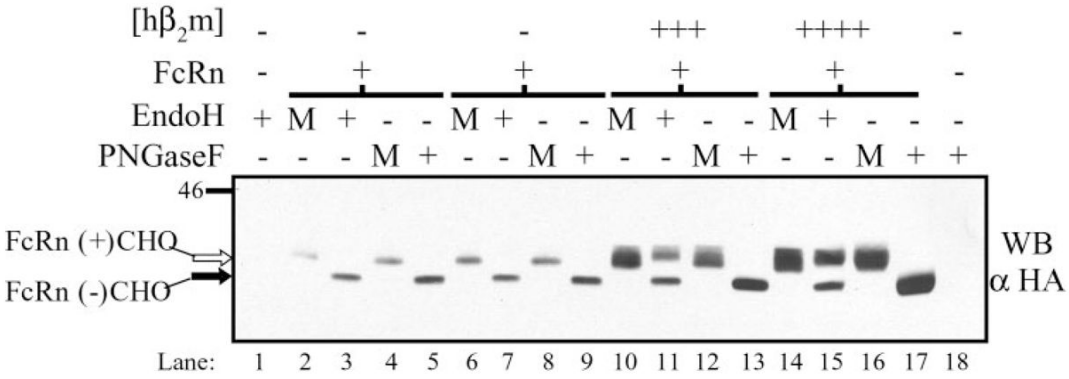

Fig. 5. Mature *N*-glycosylation is not required for IgG binding

IgG binding assays were performed as previously described using 1 mg of each clone's CHAPS lysate, at pH 6.0 only. Half of the bound proteins were either treated (+) or mock treated (*M*) with EndoH, and the other half were either treated (+) or mock treated (*M*) with PNGaseF, as previously described. Samples were then analyzed by SDS-PAGE and Western blotting for the HA tag. Samples were as follows: *lanes 1* and *18*, both empty vectors; *lanes 2–5* and *6 – 9*, FLFcRn$^{\#1}$ and pEF6/V5-HisA, two individual clones; *lanes 10 –13*, FLFcRn$^{\#1}$ and pEF6.hβ_2m (mid/high: +++); *lanes 14 –17*, FLFcRn$^{\#1}$ and pEF6.hβ_2m (high: ++++). The lysates used in this experiment are the same as those used for Fig. 4. The two clones exhibiting low and mid levels of hβ_2m expression revealed the same pattern with the amount of detectable FcRn correlating with their relative hβ_2m expression levels (data not shown). The *images* are the results of one representative experiment (n = 5). Glycosylated hFcRn (*open arrow*) and deglycosylated hFcRn (*black arrow*) are indicated. The molecular mass in kilodaltons is indicated on the *left*.

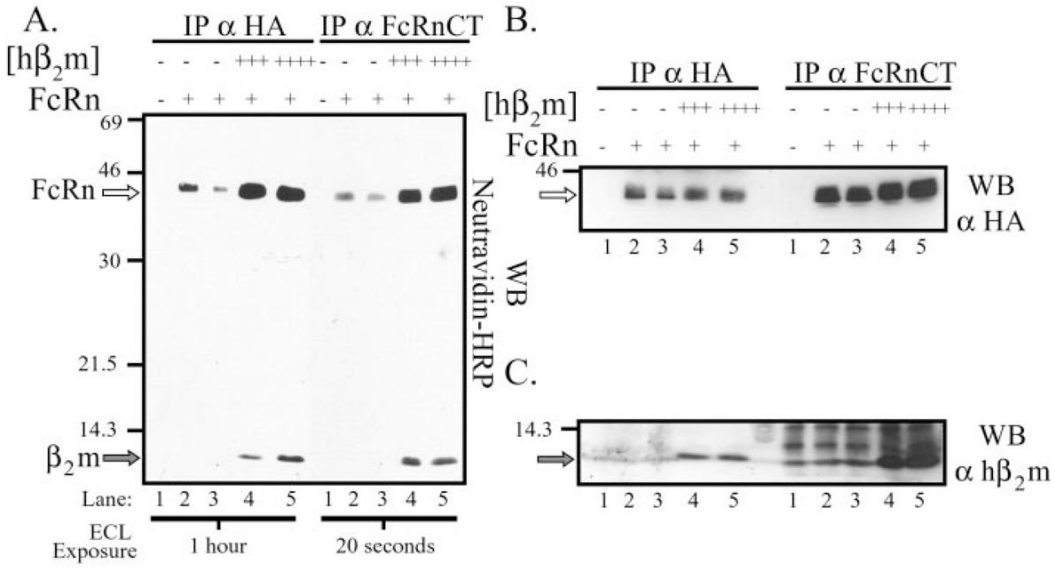

Fig. 6. Co-expressed hβ_2m greatly enhances FcRn's localization to the cell surface

A, subconfluent MDCK clones were biotinylated with the membrane-impermeant reagent, sulfo-NHS-Biotin, lysed in RIPA lysis buffer, and 350 μg of precleared lysate immunoprecipitated with 12CA5 or a rabbit anti-FcRn CT antiserum. The immunoprecipitates were analyzed by SDS-PAGE under reducing conditions and subjected to a Western blot analysis using Neutravidin-HRP. Samples were as follows: *lane 1*, both empty vectors; *lanes 2* and *3*, FLFcRn$^{\#1}$ and pEF6/V5-HisA (two clones); *lanes 4* and *5*, FLFcRn$^{\#1}$ and pEF6.hβ_2m (hβ_2m +++ and hβ_2m ++++, respectively). The 12CA5 and anti-FcRnCT immunoprecipitates were resolved on the same gel. However, due to differences in the effectiveness of the immunoprecipitations, different exposure times are shown for each (indicated at the *bottom*). The location of bands consistent with the predicted sizes of hFcRn (*open arrow*) and hβ_2m (*gray arrow*) are indicated on the *left*. *B* and *C*, the membrane from *A* was stripped and reprobed with (*B*) 12CA5 (*α-HA*) or (*C*) rabbit anti-hβ_2m as previously described to verify that *B*, FcRn was immunoprecipitated equally from all cell lysates and *B* and *C*, that the bands seen in the avidin blot were in fact FcRn and hβ_2m, respectively. The *images* are the results of one representative experiment (n = 4). *Open arrow* in *B*, hFcRn; *gray arrow* in *C*, hβ_2m. The migration of molecular mass markers is indicated at the *left* of each gel.

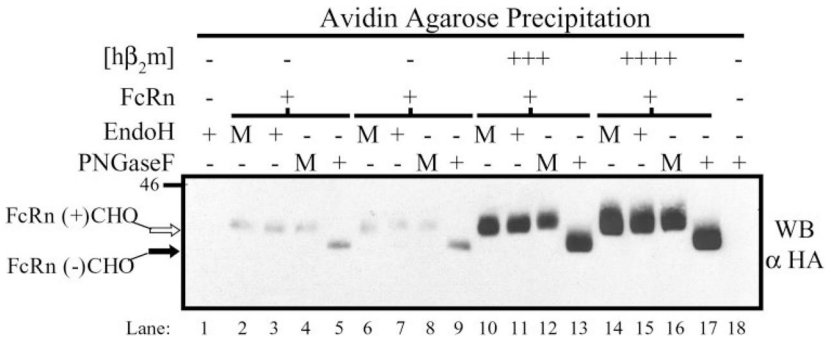

Fig. 7. Surface FcRn contains mature *N*-glycosylation

Subconfluent MDCK clones were biotinylated and harvested in RIPA lysis buffer as previously described. Surface proteins were precipitated from 1400 μg of lysate per clone by rotating gently overnight at 4 °C in the presence of avidin-agarose. Half of the bound proteins were treated (+) or mock treated (*M*) with EndoH, and the other half was treated (+) or mock treated (*M*) with PNGaseF, as previously described. Reaction products were then analyzed by SDS-PAGE and Western blotting for the HA tag. Samples were as follows: *lanes 1* and *18*, both empty vectors; *lanes 2–5* and *6–9*, FLFcRn$^{\#1}$ and pEF6/V5-HisA, two individual clones; *lanes 10–13*, FLFcRn$^{\#1}$ and pEF6.hβ_2m (mid/high: +++); *lanes 14–17*, FLFcRn$^{\#1}$ and pEF6.hβ_2m (high: ++++). The two clones exhibiting low and mid levels of hβ_2m expression revealed the same pattern with the amount of detectable surface FcRn correlating with their relative hβ_2m expression levels (data not shown). The *images* are the results of one representative experiment (n = 3). Glycosylated hFcRn (*open arrow*) and deglycosylated hFcRn (*black arrow*) are indicated. The migration of molecular mass markers is shown on the *left*.

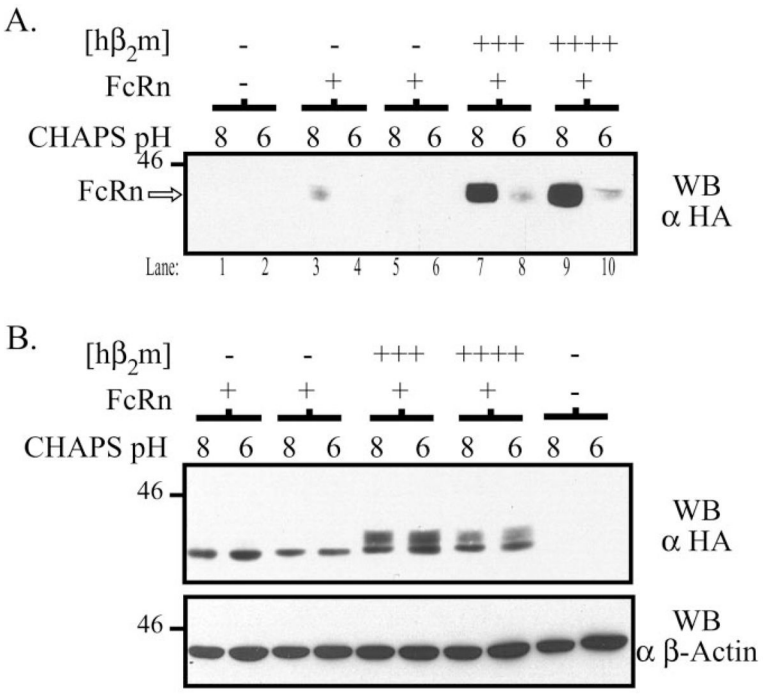

Fig. 8. Surface hFcRn in the presence of co-expressed hβ_2m is biochemically functional

A, subconfluent MDCK clones were biotinylated, lysed in 5 mg/ml CHAPS, pH 6.0 or 8.0, and an IgG binding assay was performed as previously described. The non-binding fraction of each reaction was subsequently precipitated with avidin-agarose at 4 °C overnight. The avidin precipitates were then analyzed by SDS-PAGE and Western blotting for the HA tag as previously described. Samples were as follows: *lanes 1–2*, both empty vectors; *lanes 3–4* and *5–6*, FLFcRn$^{\#1}$ and pEF6/V5-HisA, two different clones; *lanes 7–8* and *9 –10*, FLFcRn$^{\#1}$ and pEF6.hβ_2m (hβ_2m +++and hβ_2m ++++, respectively). *B*, 20 μg of each lysate was directly analyzed by Western blot for the HA tag to verify that FcRn was equally solubilized at pH 6.0 and 8.0 (*top gel*). Note the presence of a predominantly fast migrating species of hFcRn in the absence of hβ_2m and a fast and slow migrating species of hFcRn in the presence of hβ_2m consistent with an immature and mature form of hFcRn, respectively. This blot was then stripped and reprobed for β-actin. The *images* are the results of one representative experiment (n = 4). The molecular mass in kilodaltons is indicated on the *left* of each gel.

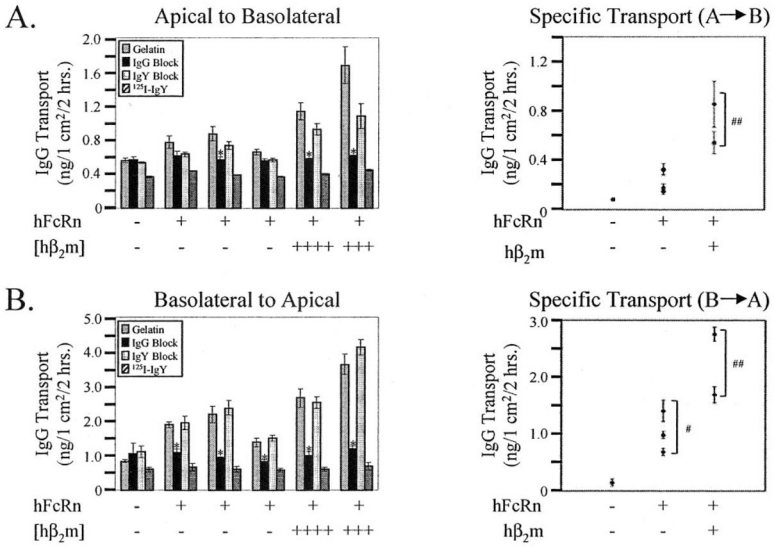

Fig. 9. Bidirectional transcytosis of IgG by hFcRn requires co-expressed hβ_2m

A control MDCK clone (hFcRn−/hβ_2m−), three clones expressing FcRn alone (hFcRn+/hβ_2m−), and the two clones co-expressing the most hβ_2m (hβ_2m +++ and ++++) were grown on Transwell filters until confluent. Following a 20-min incubation with 0.5% gelatin/HBSS+, pH 6.0, with or without a 500-fold excess of cold chicken IgY or cold human IgG on the input surface and HBSS+, pH 7.4, on the output surface, ^{125}I-IgG or ^{125}I-IgY was added to the input surface for a final concentration of 60 nM. In the latter case, ^{125}I-IgY transport in the presence of either an IgG or IgY block was not assessed. After a 2-h incubation at 37 ° C, 5% CO_2, the entire output solution was collected, precipitated with trichloroacetic acid, and the pellet counted. *A*, transcytosis of ^{125}I-IgG or ^{125}I-IgY in the apical to basolateral direction. *B*, transcytosis of ^{125}I-IgG or ^{125}I-IgY in the basolateral to apical direction. The *left histograms* for both *A* and *B* depict the mean ± S.E. (n = 3) for each experimental permutation for each clone. ANOVA, $p \leq 0.003$. The *asterisk* indicates statistical significance relative to ^{125}I-IgG in gelatin and the IgY block, but not ^{125}I-IgY at $p \leq 0.05$ by multiple comparison procedures. The *right panels* for both *A* and *B* show the mean ± S.E. (n = 3) FcRn-specific transport for each clone, calculated as follows: (^{125}I-IgG in gelatin + IgY block)/2 − (IgG Block + ^{125}I-IgY)/2. The mean ± S.E. was calculated for each group (*i.e.* hFcRn+/hβ_2m−). ANOVA p = 0.0001. #, statistical significance relative to the control MDCK clone (hFcRn−/hβ_2m−) at $p \leq$ 0.05 by multiple comparison procedures. ##, statistical significance relative to both the control MDCK clone (hFcRn−/hβ_2m−) and the MDCK clones expressing hFcRn alone (hFcRn+/hβ_2m−) at $p \leq 0.05$ by multiple comparison procedures.